Published online: 2020-03-31

Construction of Novel Bispecific Single-Domain Antibodies (BiSdAbs) with Potent Antiangiogenic Activities

Xianglei Liu[1] Tianyuan Sun[1] Qiuhan Ge[1] Jianwei Zhu[1,2,3]

[1] Engineering Research Center of Cell & Therapeutic Antibody, Ministry of Education, School of Pharmacy, Shanghai Jiao Tong University, Shanghai, China
[2] Jecho Laboratories, Inc. Maryland, United States
[3] Jecho Biopharmaceuticals Co., Ltd., Tianjin, China

Address for correspondence Jianwei Zhu, PhD, Engineering Research Center of Cell & Therapeutic Antibody, Shanghai Jiao Tong University College of Pharmacy, Ministry of Education, 800 Dongchuan Road, Shanghai 200240, China (e-mail: jianweiz@sjtu.edu.cn).

Pharmaceut Fronts 2020;2:e64–e76.

Abstract

The development of bispecific antibodies (BsAbs) has had a profound impact on cancer immunotherapy. Single-domain antibodies (SdAbs) could offer advantages over other antibody formats for the generation of a BsAbs, such as small size (~12–15 kDa), with high affinity and specificity, superior accessibility, and high yield expression in bacteria. In this study, VEGFR2 and CD16 were chosen as the targets to construct BsAbs. As the rationale, VEGFR2 is critical for tumor-associated angiogenesis, and CD16 expressed on natural killer cells is an important target on immune cells. Humanized anti-VEGFR2 SdAb 3VGR19 and anti-CD16 SdAb C21 were combined to construct several bispecific SdAbs (BiSdAbs). The biochemical properties of the BiSdAbs were characterized. They retained the high affinity for both targets, binding selectivity, and antiangiogenic activity such as inhibition of cell proliferation, migration, endothelial tube formation, angiogenesis, and cytotoxicity to cancer cells in vitro, indicating that BiSdAbs could be a potential alternative for cancer therapy.

Keywords
- bispecific antibody
- single-domain antibodies
- nanobody
- BiSdAb

Introduction

Monoclonal antibody (mAb) has been an ideal tool for targeted therapy.[1] However, long-term efficacy of mAbs was limited by resistance mechanisms, such as tumors evaded immune control.[2] Bispecific antibodies (BsAbs), such as bispecific T-cell engager (BiTE),[3] dual affinity re-targeting (DART), knob-in-hole, and bispecific antibody by protein trans-splicing (BAPTS),[4] can redirect the cytotoxic potential of immune cells to eliminate tumor cells with one arm directly engaging T cells and the other recognizing cancer cells. As it has been shown previously, additional advantages of BsAbs are that drug resistance and severe adverse effects were much reduced.[5,6] So far, three BsAbs (catumaxomab [anti-EpCAM × CD3] in 2009,[7] blinatumomab [anti-CD19 × CD3] in 2014,[8] and emicizumab [anti-Factor IXa × Factor X] in 2017,[9] have been approved for therapeutic use. The wave of next-generation "bispecific or multispecific antibodies" has arrived.[10–12]

In addition to T cells, natural killer (NK) cells are also important immune cells.[13] The ability of NK cells to quickly lyse antibody-coated tumor cells and potently secrete cytokines without prior stimulation has made NK cells ideal candidates for antigen-specific immunotherapy.[14,15] To engage NK cells, the CD16 marker on NK cells was frequently used. The anti-CD3 arm in a BiTE construct could be replaced by an anti-CD16 arm to recruit NK cells, which was called bispecific/trispecific NK cell engagers (BiKE/TriKEs).[16,17] AFM13, a tetravalent bispecific TandAb (anti-CD30 × CD16a), was developed by Affimed.[18] It was shown to induce stronger cytotoxicity toward tumor cells than an optimized anti-CD30 immunoglobulin G (IgG) or a bivalent bispecific diabody. AFM13 was in phase II clinical trials for patients with Hodgkin's lymphoma and $CD30^+$ lymphoma.[19]

It was known that angiogenesis plays an important role in the growth, invasion, and metastasis of cancer. Blockade of angiogenesis is an attractive approach to the treatment of cancer.[20] Vascular endothelial growth factors (VEGFs) and their receptors (VEGFRs) were thought to be essential regulators of angiogenesis.[21] Basic findings have shown that blocking the VEGF/VEGFR pathway could disrupt tumor micro vessels,

DOI https://doi.org/10.1055/s-0040-1708527.
ISSN 2628-5088.

inhibit tumor growth, and increase tumor oxygenation.[22] Indeed, anti-VEGF/VEGFR treatment with bevacizumab (anti-VEGF)[23] and ramucirumab (anti-VEGFR2) is currently a standard therapy for several human malignancies.[24] VEGFR2 is important for VEGF/VEGFR signaling, which is critical for tumor-associated angiogenesis and overexpressed on a variety of tumor cells. In this study, VEGFR2 was chosen as a target antigen for recognizing cancer cells.

Most of BsAbs were designed for treatment of hematological malignancies, not solid tumors. mAb has a lower accessibility in tumor tissue due to its large molecular weight. A new type of antibody, called "heavy-chain-only antibodies" (HcAbs), was discovered in 1993 from serum of *Camelidae* by the group of Hamers-Casterman.[25,26] This type of antibody is devoid of light chains, their antigen-binding or variable heavy chain domains (VHH), also named single-domain antibodies (SdAbs) or Nanobody registered by Ablynx. They retain full antigen-binding capacity.[27] Over the decades, SdAbs have received progressive interest from biopharmaceutical industry due to their unique properties, small size (~12–15 kDa), high solubility, superior cryptic cleft accessibility, low immunogenicity, deep tissue penetration, and high yield expression in bacteria or yeasts.[28,29] These properties suggest that SdAbs could offer advantages over other antibody formats for generating a BsAb.[30,31] The exciting thing is that the first nanobody drug—Cablivi (caplacizumab)—for the treatment of adults with acquired thrombotic thrombocytopenic purpura, was approved by the European Medicines Agency in 2018.[32]

Recent studies have found that VEGFR2-targeted fusion antibody (mAb04-MICA) could enhance NK-mediated immune surveillance against K562 leukemia cells through increasing degranulation and cytokine production by NK cells.[33] Moreover, mAb04-MICA was capable of reinforcing NK-cell-mediated antitumor activity in VEGFR2-expressing breast cancer both in vivo and in vitro.[34] In this study, we designed a novel BsAb, named BiSdAb. SdAbs 3VGR19 and NTV1 were generated and efficient activation of anti-VEGFR2 and inhibition of tumor cell growth were demonstrated.[35,36] Another SdAb, C21, was verified for its binding to the antigen CD16a.[37] The sequences of these SdAbs were humanized, and different combinations of BiSdAbs were constructed. The BiSdAbs were able to drive potent cell killing of VEGFR2-overexpressing cancer cells, indicating this approach as a potential alternative treatment for cancer.

Materials and Methods

Cell Lines and Proteins

Human embryonic kidney cell (HEK293T), human umbilical vein endothelial cells (HUVECs; ScienCell Research Laboratories, United States), hepatocellular carcinoma cell (BEL-7402,[38] SMMC-7721, HepG2), breast cancer cell (SK-BR-3, MCF7), and human colon cancer cell HCT-116 were used in this study. HEK293T, HepG2, and SK-BR-3 were grown in Dulbecco's modified eagle medium (DMEM, Gibco, United States), BEL-7402, SMMC-7721, HCT-116, and MCF7 were grown in Roswell Park Memorial Institute medium (RPMI 1640, Gibco), supplemented with 10% (v/v) fetal bovine serum (FBS, Gibco) and 1% (v/v) penicillin/streptomycin (P/S, Hyclone, United States). HUVECs were grown in an endothelial cell medium (ECM, ScienCell) supplemented with 10% (v/v) FBS, 1% (v/v) endothelial cell growth supplement (ECGS), and 1% (v/v) P/S provided by the manufacturers. HUVECs at passage 4–5 were used in this research. An FcγRIIIa (CD16a)-transfected NK92 cell (NK92-FcR cell)[34] was cultured in MEM Alpha medium, supplemented with 12.5% FBS (Hyclone, Australia), 12.5% (v/v) horse serum (Hyclone), 0.1 mmol/L 2-mercaptoethanol, 0.2 mmol/L myo-inositol (Sigma-Aldrich, St. Louis, Missouri, United States), 0.02 mmol/L folic acid (Sigma-Aldrich), and 200 U/mL hIL-2 (Millipore, United States). Peripheral blood mononuclear cells were isolated from human fresh blood, then cultured in ALyS505NK-AC&EX medium (CSTI, Japan), supplemented with 1,000 U/mL hIL-2 for 14 days to enrich NK cells. All the cultures were maintained in a plastic flask and incubated at 37 °C in 5% CO_2.

Recombinant human VEGFR2 was purchased from ProSpec (Israel). VEGFR2 antibody (2C6) was purchased from Novus Biologicals (United States). Recombinant human CD16a, $VEGF_{165}$, PE-conjugated VEGFR2 antibody, FITC-conjugated CD3 antibody, and APC-conjugated CD56 antibody were purchased from Sino Biological (Beijing, China). Peroxidase-conjugated goat anti-mouse immunoglobulin G (IgG) was purchased from Jackson Immuno (United States). CD16a mAb (3G8), FITC-conjugated rat anti-mouse IgG1 secondary antibody, and FITC-conjugated 6 × His tag mAb (AD1.1.10) were purchased from Thermo Fisher (United States). His-probe (H-3) was purchased from Santa Cruz (United States). Akt (pan) (C67E7) rabbit mAb #4691, p38 MAPK (D13E1) XP rabbit mAb #8690, p44/42 MAPK (Erk1/2) (137F5) rabbit mAb #4695, phospho-Akt (Ser473) (D9E) XP rabbit mAb #4060, phospho-p38 MAPK (Thr180/Tyr182) (D3F9) XP rabbit mAb #4511, phospho-p44/42 MAPK (Erk1/2) (Thr202/Tyr204) (D13.14.4E) XP rabbit mAb #4370, phospho-VEGFR2 (Tyr1175) (19A10) rabbit mAb #2478, and horseradish peroxidase (HRP)-linked anti-rabbit IgG antibody #7074 were purchased from Cell Signaling Technology (United States). GAPDH rabbit antibody was purchased from Yeasen (Shanghai, China).

Humanization of SdAb

SdAb sequences of 3VGR19, NTV1, and C21 were published before.[35–37] The complementarity-determining regions (CDRs) were analyzed by IMGT, the international ImMunoGeneTics information system (http://www.imgt.org).[39] These *Camel* source SdAbs were humanized by two methods. The first one is CDR grafting using a universal humanized SdAb scaffold by Vincke and collaborators.[40] The second is the classical CDR grafting according to the protocol.[41] SWISS-MODEL (http://swissmodel.expasy.org) was used for modeling protein tertiary and quaternary structures.[42]

Expression and Purification of SdAbs

The genes of parental, humanized SdAbs and BiSdAbs were synthesized by Synbio Technologies (Soochow, China), then cloned into plasmid pET-22b(+) between restriction sites *Nco*I and *Xho*I. The vector pET-22b(+) contains PelB signal peptide, leader sequence at the *N*-terminus for periplasmic

localization in *Escherichia coli*, and 6 × His-tag at the *C*-terminus for protein purification.

The recombinant plasmids were transformed in *E. coli* BL21 (DE3) competent cells and plated on Luria-Bertani (LB) agar plates supplemented with 100 μg/mL ampicillin. After an overnight incubation, fresh colonies inoculated in 5 mL terrific broth (TB) medium, then scaled up bacterial culture from 5 mL to 1 L in a shaker incubator at 37 °C until the OD_{600} reached to 0.6 and then induced with 1 mmol/L isopropyl-β-*D*-thiogalactopyranoside (IPTG). After induction, cells were allowed to grow and express for 20 hours at 30 °C before harvesting the cell pellet by centrifugation at approximately 8,000 × *g* for 10 minutes.

The periplasmic proteins were extracted by osmotic shock[43] and purified by nickel affinity chromatography (Ni^+-NTA) (GenScript, Nanjing, China). This periplasmic extract was loaded on a His-Select column (Sigma-Aldrich). After washing with phosphate-buffered saline (PBS), the proteins were eluted with 100 to 300 mmol/L imidazole and concentrated on Amicon Ultra-3K centrifugal filter devices (Millipore) with a molecular mass cutoff of 3 kDa. The purity of the protein was evaluated in a Coomassie Blue stained 15% SDS-PAGE and Western blotting with anti-His tag mouse antibody and the goat anti-mouse IgG-HRP conjugate antibody. A broad-range protein marker (Fermentas) was used as a molecular weight indication. The final yields of SdAbs were determined through a BCA protein assay kit (Beyotime, Shanghai, China).

Surface Plasmon Resonance Kinetics Measurements

Affinity constants for the binding between SdAbs and VEGFR2 or CD16a were determined by surface plasmon resonance (SPR) analysis using the Biacore T200 analytical system (GE Healthcare). The VEGFR2 or CD16a was immobilized on the CM-5 sensor chip. After immobilization, an interaction analysis with different samples was performed at 25 °C with PBS-0.5% (v/v) Tween-20 as running buffer, and the SdAbs were diluted in PBS to concentrations between 5 and 1,000 nmol/L and injected at a flow rate of 30 μL/min. Parental SdAbs 3VGR19 and C21 were used to optimize this process. After each cycle, the chip was regenerated with 20 μL of 100 mmol/L Gly-HCl solution. All Biacore kinetics experimental data were obtained using the Biacore T200 evaluation software to estimate the association rate constant (k_a) and dissociation rate constant (k_d). Data from the three experimental flow cells of a single biosensor chip were globally fit to a 1:1 bimolecular binding model. The equilibrium dissociation constant (K_D) was calculated from the ratio k_d/k_a. To determine whether BiSdAbs bind VEGFR2 and CD16a simultaneously, the first antigen VEGFR2 was immobilized on the CM-5 sensor chip, then BiSdAb was injected, and the response value increased. The second antigen CD16A was injected subsequently after the first equilibrium and the response value increased again.

Flow Cytometry Analysis

The VEGFR2 expressing HUVEC cells. HUVECs and the VEGFR2-negative cell HEK293, CD16a-transfected NK92-FcR cell were used for fluorescence-activated cell sorting (FACS) analysis. The cells were harvested and washed three times with PBS-1% bovine serum albumin (BSA; w/v); ~3×10^5 cells were resuspended in a total volume of 100 μL. Parental SdAbs 3VGR19 and C21 were used as positive control. One microgram of SdAb was added, and cells were incubated for 30 minutes on ice. After washing three times with PBS-1% BSA (w/v), the cells were incubated with 1 μg mouse anti-His-tag FITC conjugate antibody for 30 minutes on ice. Excess fluorescein-labeled antibody was removed by washing with PBS-1% BSA (w/v) and the cells were finally resuspended in 500 μL PBS-1% BSA (w/v) and analyzed on a Beckman CytoFlex (United States).

CCK-8 Cell Proliferation Assay

Cell Counting Kit-8 (Dojindo, Shanghai, China) was used following the protocol of the manufacturer. Briefly, HUVECs (2.5×10^3 cells/well) were plated onto 96-well tissue culture plates in 50 μL 2% FBS (v/v)-ECM medium without ECGS and incubated at 37 °C for 2 hours. SdAbs at the indicated concentrations or vehicle were mixed with 40 ng/mL $VEGF_{165}$ at a final volume of 50 μL and added to each well, and incubated for an additional 72 hours. At the end of incubation, 10 μL CCK-8 was added to each well, and the color development was measured by reading the absorbance at 450 nm using the microplate reader Infinite M200 PRO (TECAN). The cell survival rate (%) of target cells was calculated using the following formula: $[(A_s–A_b)/(A_0–A_b)] \times 100\%$, where A_s, A_b, and A_0 are the absorbent values of the sample group, medium, and measurement group at 0 nmol/L, respectively. The IC_{50} values were then calculated by curve fitting using GraphPad Prism software (San Diego, United States).

Wound Healing Assay (Scratch Assay)

A total of 2×10^5 HUVECs were placed into a 24-well plate and then starved by serum-free ECM for 12 hours. The monolayer cells were scratched with a 200-μL pipette tip and washed twice with PBS to remove debris. The cell monolayer was then maintained in serum-free ECM and cultured for further 24 hours, and different concentrations of Abs were added with or without 40 ng/mL $VEGF_{165}$. Images were taken with an inverted light microscope (NIKON ECLIPSE Ti-S,TS-100). The wound migration rates (%) were measured with Image J software and calculated as follows: $(S_0–S_{time})/S_0 \times 100\%$.

Endothelial Tube Formation Assay (In Vitro Angiogenesis)

Geltrex LDEV-Free Reduced Growth Factor Basement Membrane Matrix (Invitrogen) was thawed on ice for 24 hours, and 50 μL aliquots were transferred to a 96-well tissue culture plate and incubated at 37 °C for 1 hour to solidify. For the assays, ~2×10^4 HUVEC cells suspended in 100 μL 2% FBS-ECM, with or without anti-VEGFR2 SdAbs at indicated concentrations, were seeded onto the surface of the polymerized Geltrex and incubated at 37 °C overnight in a CO_2 incubator. The following day endothelial tube formation was

digitally photographed under an inverted light microscope (NIKON ECLIPSE Ti-S, TS-100). Branching structure analysis was performed to evaluate the performance of SdAbs. For branching structure analysis, the branched points in the control well (cells treated with $VEGF_{165}$) were counted and defined as 100% branching. Then the branched points in groups were counted and placed in the following equation: branching/% = counted branch point in each group/counted branch point in control well × 100%. Image J analysis was performed to analyze quantitatively the tube formation procedure.

Apoptosis Assay

HUVECs were incubated with various treatments at 37 °C for 48 hours, and then stained with annexin V-FITC and propidium iodide (PI) to distinguish populations of early apoptotic (annexin V^+/PI^-), late apoptotic (annexin V^+/PI^+), and necrotic (annexin V^-/PI^+) using annexin V/PI Apoptosis Assay Kit (BD Pharmingen). The percentage of apoptotic cells was calculated as the sum of the percentages of early apoptotic and late apoptotic cells.

Immunoblotting Assay

The effect of BiSdAb (C21–1 + 3VGR19–3) was examined on tyrosine phosphorylation of VEGFR2 and downstream signal proteins AKT/ERK/P38 MAPK. HUVECs were starved for 24 hours in a six-well plate, and then treated with series of concentrations for 1 hour, followed by stimulation with 40 - ng/mL VEGF for another hour. The whole cell extracts were harvested using RIPA buffer (Beyotime, Shanghai, China). Proteins were resolved by electrophoresis and then transferred onto polyvinylidene fluoride (PVDF) membranes. The membranes were blocked and incubated with primary antibodies at 4 °C overnight. After washing, the membranes were incubated with the corresponding secondary anti-mouse/anti-rabbit antibodies conjugated to HRP. The membranes were reacted with enhanced enhanced chemiluminescence reagent (Millipore) and exposed using a Bio-Rad detection system. The relative expression level was quantified according to the reference protein GAPDH. Image J software was used for gray scanning.

NK Cell Cytotoxicity Assay

CytoTox 96 Non-Radioactive Cytotoxicity Assay Kit (Promega, United States) was used following the protocol of the manufacturer. Briefly, BEL7402 (1×10^4 cells/well) cells were plated onto 96-well tissue culture plates in 100 µL 5% FBS (v/v)-1640 medium without phenol red and incubated at 37 °C for 12 hours. SdAbs/BiSdAb and NK cells with an effect: target ratio (E:T = 10:1) were added and incubated for an additional 16 hours. A triplicate set of wells for the culture medium background without cells, effector cell spontaneous lactate dehydrogenase (LDH) release, and target cell spontaneous LDH release group was prepared. At the end of incubation, 22 µL 10% Triton X-100 was added to target maximum wells. The supernatants were transferred to a new 96-well plate, CytoTox 96 reagents were added to each well, and the color development was measured by reading the absorbance at 490 nm using the microplate reader Infinite M200 PRO (TECAN). The cell cytotoxicity rate (%) of target cells was calculated using the following formula: cytotoxicity/% = (experimental – effector spontaneous – target spontaneous)/(target maximum – target spontaneous) × 100%. Data were analyzed using GraphPad Prism software (San Diego, United States).

Statistical Analysis

All experiments were conducted in triplicate, and data were averaged and presented as the mean ± standard deviation. Significant differences were determined by one-way analysis of variance followed by Tukey's test, using the SPSS (version 20.0) package. Statistical significance was defined as $p < 0.05$.

Results

Humanization of SdAb

For therapeutic applications, the camelid-specific amino acid sequences in the framework (FR) have to be mutated to their human heavy-chain variable domain equivalent, i.e., humanization.[40,44] The structure of variable heavy chain domain of human (VH) and *Camelidae* (VHH) were highly similar, with a homology between 80 and 90%, in which 10 amino acids are different.[45]

Vincke and collaborators described an universal humanized SdAb scaffold in 2009, which allows grafts of antigen-binding loops from other SdAbs with transfer of the antigen specificity and affinity.[40] This universal scaffold was used as the first humanization method, the CDRs (analyzed by IMGT) of the parental SdAbs 3VGR19, NTV1, and C21 were genetically grafted to h-$NbBcII10_{(FGLA)}$, and the candidates were named 3VGR19–1, NTV1–1, and C21–1, respectively.

The second method was classical CDR grafting, which means grafting the CDRs of SdAb into the homologous human antibody variable region.[46] Notably, critical *Camelidae* framework residues need to be reintroduced as back mutations to restore the optimum CDR conformations for antigen binding.[41] We named these new SdAbs as 3VGR19–2–5, NTV1–2, and C21–2, respectively.

The detailed amino acid sequence is shown in ►**Fig. 1A**, and their spatial structure diagrams were obtained based on different templates (3kdm.2.B for NTV1 and variants, 5iml.1.B for C21 and its variants, 3eak.1.A for 3VGR19 and its variants) using SWISS-MODEL (►**Supplementary Fig. S1** [online only]). Preliminary results show that the differences of the spatial structure between candidates and parental SdAbs were minimal. The conformations and main-chain structures were consistent. Sequence homology of all humanized SdAbs compared with the templates was between 67 and 81% (►**Table 1**).

Expression and Purification of SdAbs and BiSdAbs

Escherichia coli is a simple host system to express SdAbs and BiSdAbs. For the expression and purification, all genes of interest were synthesized and subcloned into the vector pET-22b(+). The sequence of the construct and surrounding expression region was confirmed by DNA sequencing.

SdAbs were secreted to the periplasms of *E. coli*, fused with a His tag for purification by immobilized metal-ion

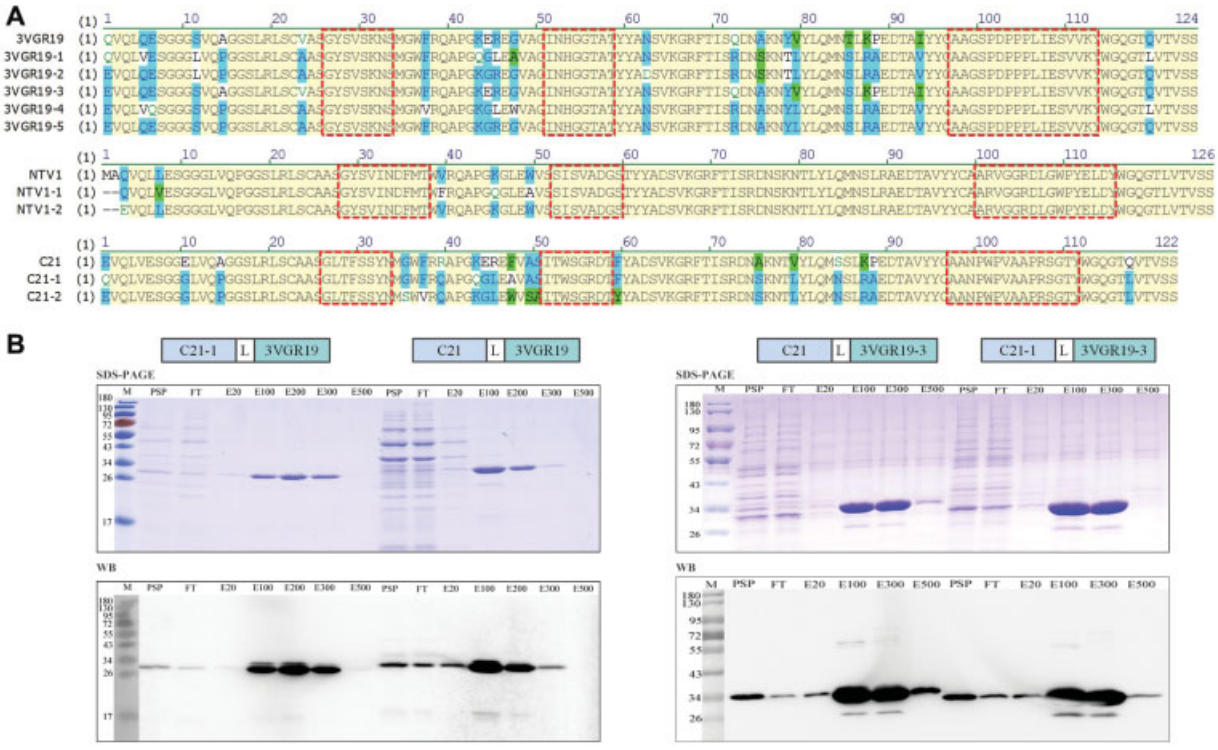

Fig. 1 (A) Alignment of amino acid sequences of SdAbs. 3VGR19, NTV1, and C21 are the parental SdAbs, others are humanized SdAbs. Complementarity determining regions (CDRs) of the variable domain (analyzed by IMGT) are indicated by *red boxes*. The mutant amino acids are shown in color background. (**B**) Schematic construct purification and identification of BiSdAbs. The purity of the proteins was determined using Coomassie-stained 15% SDS/PAGE. The Abs were verified by Western blot (WB) with anti-His antibodies. The revealed bands of ~28 kDa correspond to the BiSdAbs. L is $(G_4S)_3$ linker, M is size standards. PSP means the periplasmic space protein, FT is flow-through by IMAC, E20–E500 are elution samples with 20–500 mmol/L imidazole.

Table 1 Sequence homology of SdAbs compared with different templates using SWISS-MODEL

3kdm.2.B	NTV1	NTV1–1	NTV1–2	5iml.1.B	C21	C21–1	C21–2
100%	80.33%	78.69%	81.15%	100%	81.15%	76.23%	75.41%
3eak.1.A	3VGR19	3VGR19–1	3VGR19–2	3VGR19–3	3VGR19–4	3VGR19–5	
100%	67.74%	81.45%	77.42%	73.98%	73.98%	74.19%	

affinity chromatography (IMAC). SdAbs present as a single band of ~14 kDa. The purity of the protein was more than 95% after purification (►**Supplementary Fig. S2** [online only]). BiSdAbs were constructed by linking two SdAbs, anti-VEGFR2, and anti-CD16a, with a $(G_4S)_3$ linker. The recombinant protein presents as a single band of ~28 kDa. The purified BiSdAbs were confirmed to be His-tagged Abs by Western blotting (►**Fig. 1B**). An average yield of approximately 5 to 30 mg purified protein was obtained per liter of overnight culture in baffled shake flasks.

Characterization of SdAbs and BiSdAbs

Evaluation of the binding antigens VEGFR2 and CD16a with SdAbs was performed by SPR analysis. The sensorgram curves are shown in ►**Fig. 2A**. Data from three experimental flow cells of a single biosensor chip were globally fit to a 1:1 bimolecular binding model and detailed kinetic parameters are listed in ►**Table 2**. A higher affinity with VEGFR2 was observed for 3VGR19 ($K_D = 2.7$ nmol/L) compared with NTV1 ($K_D = 595.1$ nmol/L). Finally, we obtained humanized SdAbs 3VGR19–3 ($K_D = 2.1$ nmol/L), which showed higher affinity (0.78-fold) than the parental SdAb 3VGR19 ($K_D = 2.7$ nmol/L), while for the target CD16a, humanized SdAb C21–1 ($K_D = 2.9$ nmol/L) showed 4.83-fold lower affinity than the parental SdAb C21 ($K_D = 0.6$ nmol/L). Therefore, we continued further experiments with 3VGR19, 3VGR19–3, C21, and C21–1, to construct four BiSdAbs.

The affinity of BiSdAbs to antigens VEGFR2 and CD16a were also verified by SPR. The sensorgram curve showed that BiSdAbs had a comparable or higher affinity than VEGFR2 ($K_D = 0.1$–4.7 nmol/L, the best decreased by 0.04-fold) and CD16a ($K_D = 0.5$–2.9 nmol/L, the best decreased by 0.82-fold) compared with the parental monomeric SdAb 3VGR19 ($K_D = 2.7$ nmol/L) and C21 ($K_D = 0.6$ nmol/L), respectively (►**Fig. 2B** and ►**Table 2**). Otherwise, different combinations of these four SdAbs showed similar affinity. These SPR results showed that the construction of BiSdAbs was better on antigen recognition compared with the

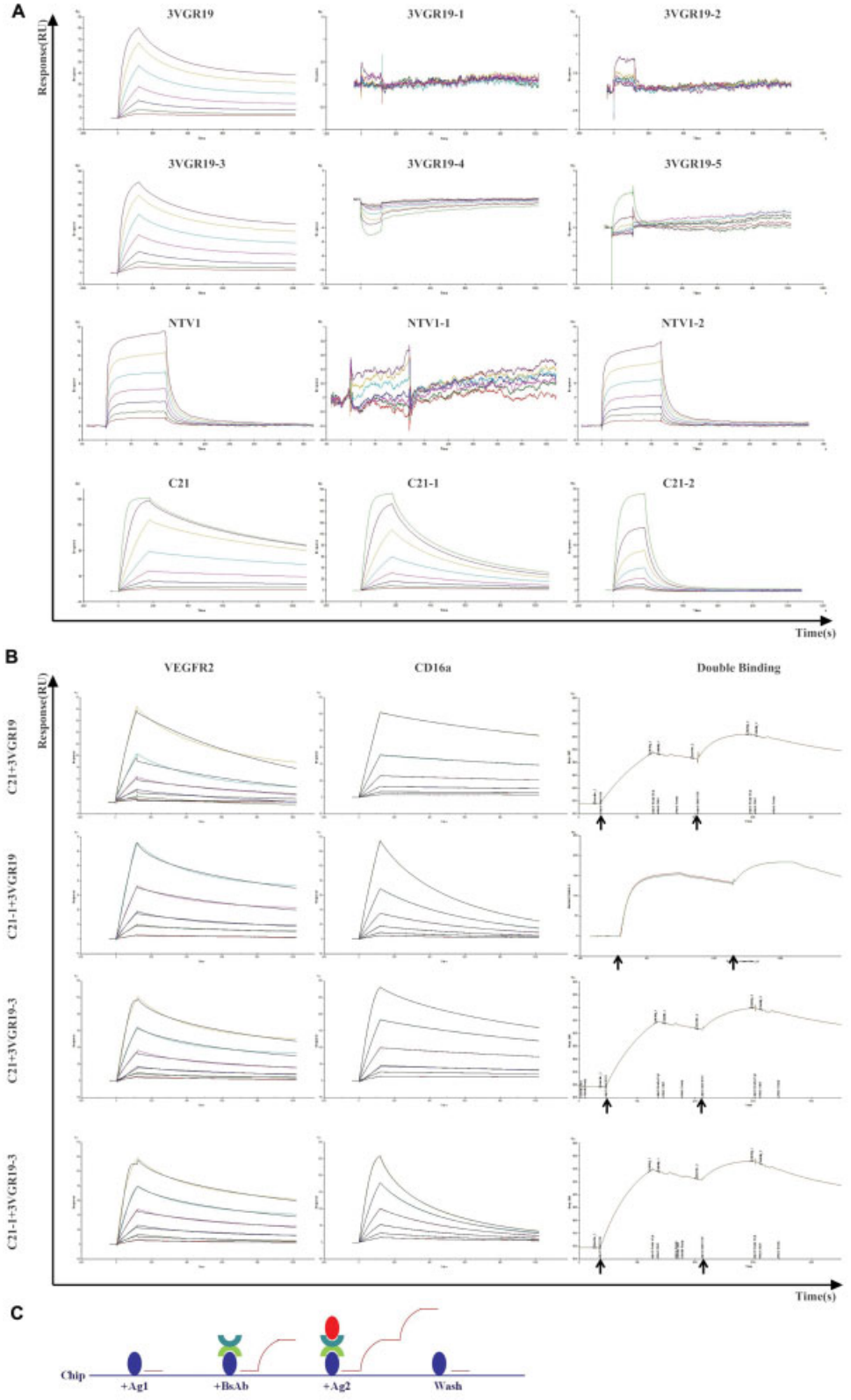

Fig. 2 Set of sensor grams of SdAbs (**A**) and BiSdAbs (**B**) binding with VEGFR2 or CD16a by SPR analysis. Data from three experimental flow cells of a single biosensor chip were globally fit to a 1:1 bimolecular binding model and are summarized in ►**Table 2**. (**C**) Schematic diagram of double binding experiments. The first antigen VEGFR2 was immobilized on a CM-5 sensor chip, the BiSdAb was then injected (first arrow in B); the response value increased. The second antigen CD16A was injected (second arrow in B) subsequently after the first equilibrium and the response value increased again. SPR, surface plasmon resonance.

Table 2 Kinetic rate and equilibrium binding constants of the SdAbs and BiSdAbs measured by SPR

Abs	Targets	k_a (1/Ms)	k_d (1/s)	K_D (mol/L)	Relative value than parental SdAb (3VGR19/C21)	
NTV1	VEGFR2	$7.109E^{+4}$	0.04230	$5.951E^{7}$	218	/
NTV1–1	VEGFR2	/	/	/	/	/
NTV1–2	VEGFR2	$5.462E^{+4}$	0.04005	$7.2332E^{7}$	265	/
3VGR19	VEGFR2	$3.593E^{+5}$	$9.800E^{4}$	$2.728E^{9}$	1	/
3VGR19–1	VEGFR2	/	/	/	/	/
3VGR19–2	VEGFR2	/	/	/	/	/
3VGR19–3	VEGFR2	$3.277E^{+5}$	$7.006E^{4}$	$2.138E^{9}$	0.78	/
3VGR19–4	VEGFR2	/	/	/	/	/
3VGR19–5	VEGFR2	/	/	/	/	/
C21	CD16a	$2.685E^{+6}$	0.001630	$6.069E^{10}$	/	1
C21–1	CD16a	$2.076E^{+6}$	0.006090	$2.934E^{9}$	/	4.83
C21–2	CD16a	$6.089E^{+5}$	0.05134	$8.430E^{8}$	/	138.9
C21 + 3VGR19	VEGFR2	$2.463E^{+5}$	0.001175	$4.772E^{9}$	1.75	/
C21–1 + 3VGR19	VEGFR2	$1.014E^{+8}$	0.01138	$1.123E^{10}$	0.04	/
C21 + 3VGR19–3	VEGFR2	$7.702E^{+6}$	0.004344	$5.639E^{10}$	0.21	/
C21–1 + 3VGR19–3	VEGFR2	$8.033E^{+6}$	0.003256	$4.053E^{10}$	0.15	/
C21 + 3VGR19	CD16a	$7.204E^{+6}$	0.003600	$4.998E^{10}$	/	0.82
C21–1 + 3VGR19	CD16a	$5.033E^{+7}$	0.07950	$1.580E^{9}$	/	2.6
C21 + 3VGR19–3	CD16a	$2.625E^{+6}$	0.001394	$5.310E^{10}$	/	0.88
C21–1 + 3VGR19–3	CD16a	$3.126E^{+6}$	0.009237	$2.954E^{9}$	/	4.87

Note: The association and dissociation constants (k_a and k_d) were calculated using Biacore T200 Evaluation software. K_D was calculated from the quotient of k_d/k_a. The symbol "/" indicates not detected.

monovalent SdAb. Through the double binding experiments (SPR), the response value increased twice, thus these BiSdAbs bound VEGFR2 and CD16a simultaneously (►**Fig. 2B**) as they were designed.

In addition, the ability of SdAbs and BiSdAbs for the recognition of receptors on a cell surface was analyzed by flow cytometry. First, to choose a suitable cell line, the expression level of VEGFR2 was evaluated in different cell lines including HEK293T, HUVECs, hepatocellular carcinoma cells (BEL-7402, SMMC-7721, HepG2), breast cancer cells (SK-BR-3, MCF7), and human colon cancer cell line HCT-116. The results (►**Supplementary Fig. S3** [online only]) showed that the signal was significantly shifted with HUVECs as indicated using a positive control antibody 2C6, while the signal was marginally shifted with BEL-7402 due to low expression of VEGFR2. Nevertheless, they were used as positive cells in the following experiments, while HEK293T without VEGFR2 was used as a negative control.

The affinities of SdAbs and BiSdAbs were then evaluated. Antibodies 2C6 and 3G8 were used as positive controls that bind to VEGFR2 and CD16a, respectively. For HEK293 cells, the signal was not shifted as expected. For HUVEC and BEL-7402 cells, 3VGR19 and 3VGR19–3 showed stronger signal shifts than either NTV1, NTV1–2, or 2C6. For NK92-FcR cells, C21 and C21–1 showed a moderate shift. These results indicate that 3VGR19 and 3VGR19–3 effectively recognized the antigen VEGFR2 on HUVECs and BEL-7402 cells, while C21 and C21–1 recognized CD16a on NK92-FcR cells, respectively (►**Fig. 3A**). Furthermore, FACS analysis showed the binding capacity of all the BiSdAbs to human VEGFR2 on HUVECs and the BEL-7402 cell surface (►**Fig. 3B**), and CD16a on the NK92-FcR cell surface (►**Fig. 3C**).

Biological Activities of SdAbs and BiSdAbs

Biological activities such as inhibition of cell proliferation, migration, endothelial tube formation, and induction of cell apoptosis were verified. Inhibition of cell proliferation may indicate a possibility for cancer treatment. We measured cell viability in HUVEC cells treated with different concentrations of SdAbs or BiSdAbs using CCK-8 assays. As shown in ►**Fig. 4A**, SdAbs and BiSdAbs inhibited HUVEC cell proliferation in a dose-dependent manner. Through calculation by curve fitting using GraphPad Prism software, IC_{50} values shown by BiSdAbs were approximately 5.9 to 13.4 nmol/L, while IC_{50} shown by SdAbs appeared much higher, around 570.7 to 751.5 nmol/L, than those of BiSdAbs. These results indicate that BiSdAbs had stronger inhibition effects on HUVEC proliferation, which correlates well with the results of BiSdAbs' higher affinity than that of the parental SdAbs.

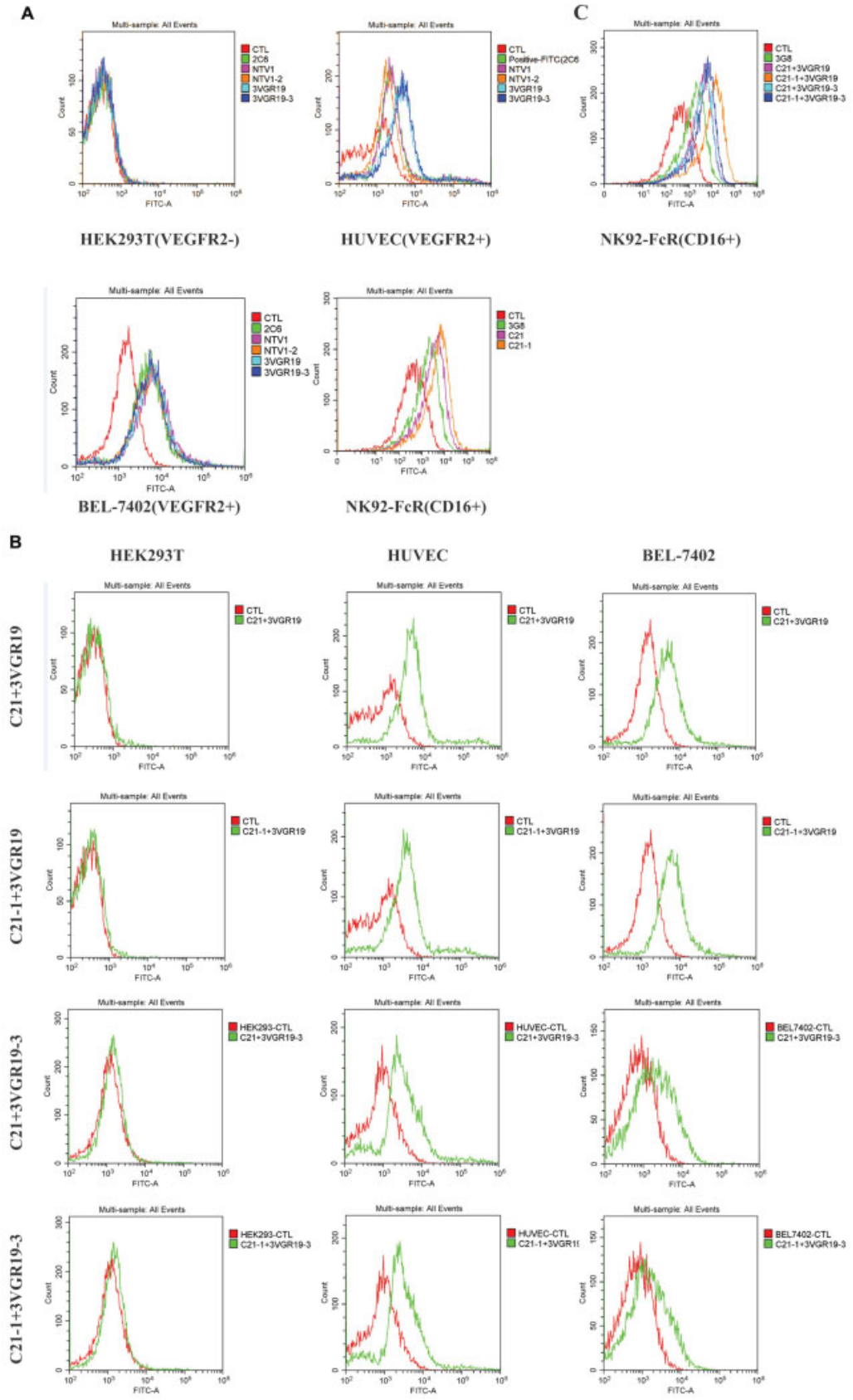

Fig. 3 Flow cytometry analysis of SdAb (**A**) or BiSdAb (**B** and **C**) binding to VEGFR2 or CD16a antigen on the cell surface. HEK293T, VEGFR2-negative cells; HUVEC and BEL-7402, VEGFR2-positive cells; NK92-FcR, NK92 cells transfected with FcγRIIIa (CD16a). Cell lines were incubated with SdAbs or BiSdAbs and detected with anti-His FITC conjugate Abs. A total of 35,000 cells were analyzed and PBS was used as negative control. 2C6 and 3G8 are anti-VEGFR2 and anti-CD16a-positive antibodies, respectively.

Given that endothelial cell migration is essential for angiogenesis, we performed wound healing assays to investigate the effect of SdAbs and BiSdAbs on HUVEC migration. As shown in ►**Fig. 4B**, most of the scratches in control groups were covered by cells after 24 hours, while the presence of 20 nmol/L 3VGR19–3 or C21–1 + 3VGR19–3 strongly inhibited HUVEC migration (27.82% or 38.03% vs. 74.02%, $p < 0.05$). For BEL-7402 cells, the results were the same (►**Supplementary Fig. S4** [online only]). Migration rates of 3VGR19, 3VGR19–3, and C21–1 + 3VGR19–3 were 18.75, 28.59, and 15.90%, respectively, compared with the control group of (48.57%, $p < 0.05$). These results indicate that BiSdAbs inhibit HUVEC and BEL-7402 migration.

Although angiogenesis is a complicated process involving several types of cells, tube formation by endothelial cells is one of the key steps. HUVECs were grown on matrigel in the presence of 20 nmol/L 3VGR19–3 and C21–1 + 3VGR19–3. The ability of tube forming capillary was examined. As shown in ►**Fig. 5A**, after overnight incubation, fewer capillary tubes were formed by HUVECs grown in the presence of 3VGR19–3 and C21–1 + 3VGR19–3. The number of nodes was counted as 77.63 and 76.06% in the presence of 3VGR19–3 and C21–1 + 3VGR19–3 respectively as that of the control ($p < 0.05$). Thus, treatment with 3VGR19–3 and C21–1 + 3VGR19–3 showed antiangiogenic effects on HUVECs.

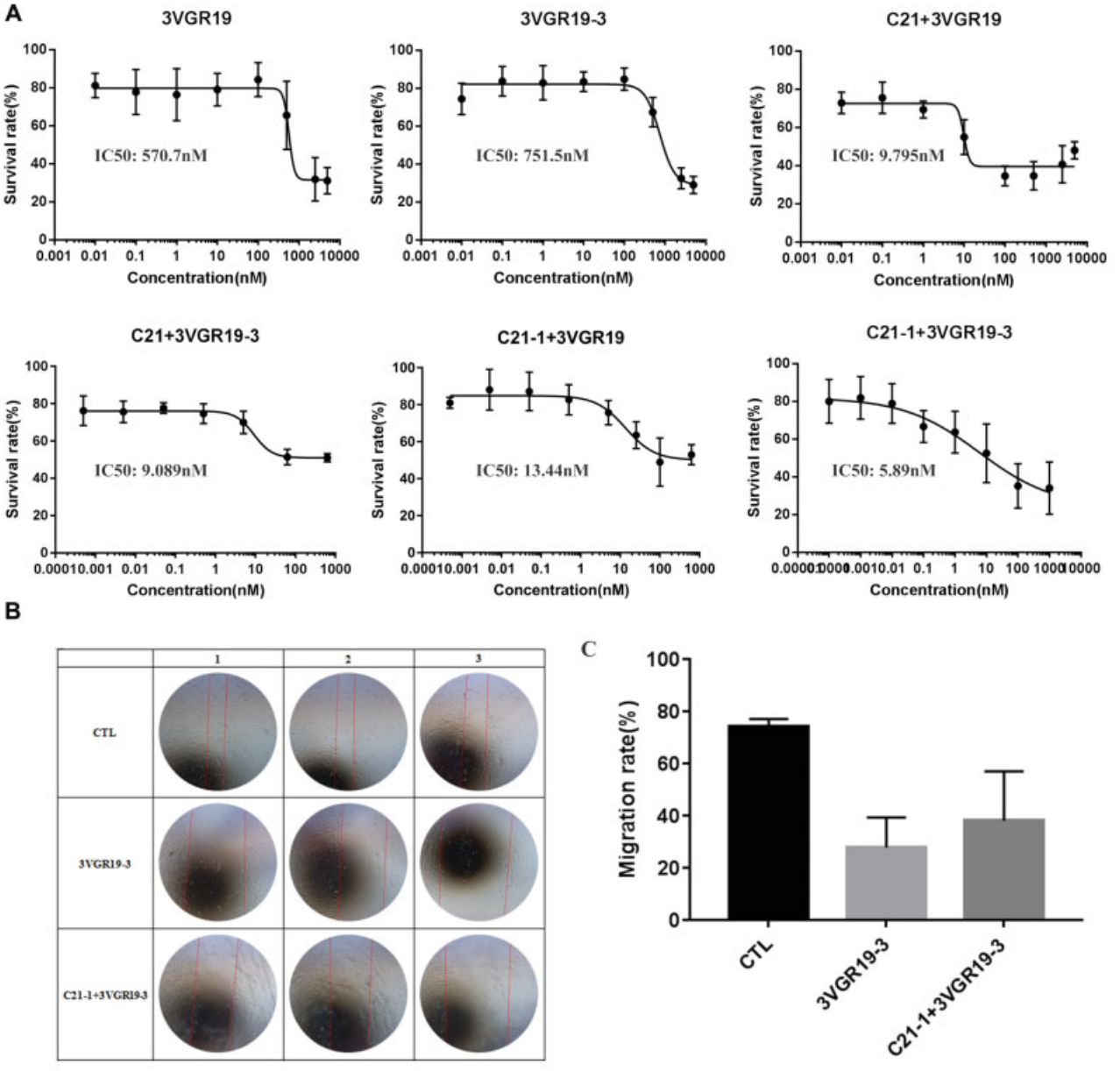

Fig. 4 Bioactivity of the BiSdAbs, proliferation inhibition and migration of HUVECs. (**A**) SdAbs or BiSdAbs inhibited the proliferation of HUVECs with VEGF stimulated in a dose-dependent manner. A CCK-8 assay was performed on HUVECs (2.5×10^3 cells/well). The IC_{50} values were calculated by curve fitting using GraphPad Prism software. (**B**) HUVECs were wound using pipette tip and then treated with SdAbs or BiSdAbs (24 hours). (**C**) Migrated distances were quantified by Image J software and the wound migration rates (%) were calculated as follows: $(S_0 - S_{time})/S_0 \times 100\%$. The data represent the mean of the triplicate experiments.

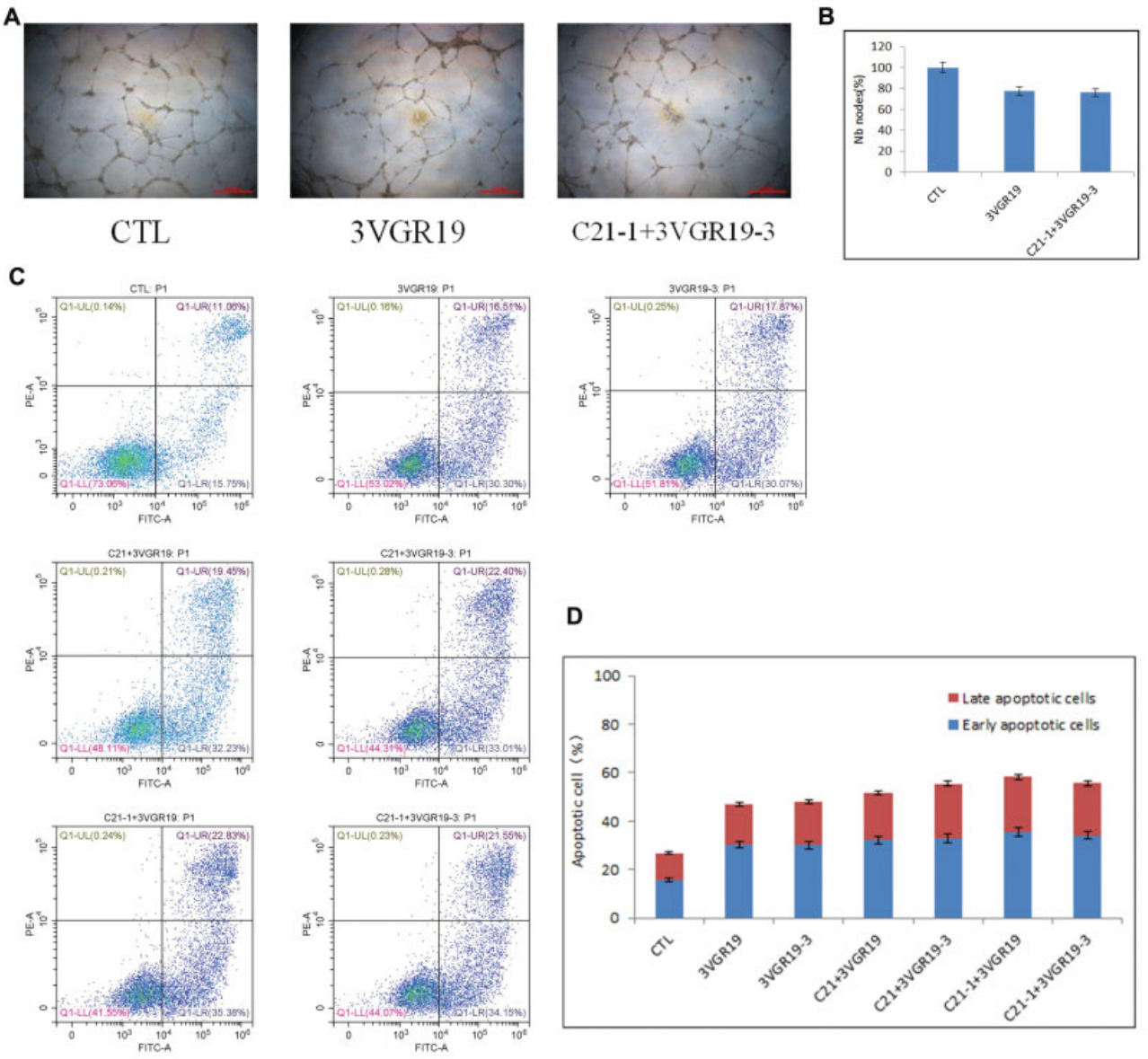

Fig. 5 BiSdAbs inhibited tube formation and induced apoptosis of HUVECs. (**A** and **B**) HUVECs' tube-like photomicrographs and quantitative analysis demonstrated the significant effects of SdAbs or BiSdAbs on HUVECs tube formation. Numbers of nodes and total branching length were quantified by Image J software. (**C** and **D**) HUVECs were incubated with various treatments at 37 °C for 48 hours and analyzed by flow cytometry following staining with Annexin V-FITC and PI. The percentage of cells in each quadrant is indicated, and the proportions of early apoptotic cells (Annexin V-positive) and late apoptotic cells (PI-positive) are shown. The data represent the mean of the triplicate experiments. PI, propidium iodide.

As another functional assay, cytotoxicity was analyzed by annexin V/PI staining. As shown in ►**Fig. 5B**, 3VGR19 or 3VGR19–3 decreased the percentage of proliferating HUVEC cells by 20% (from 73.06 to 53.02% or 51.81%). Treatment with BiSdAbs markedly increased apoptosis of HUVEC cells from 26.81% (early apoptosis: 15.75% plus late apoptosis: 11.06%) to 51–58% ($p < 0.05$). These observations collectively suggest strong inhibition of angiogenesis in vitro by BiSdAbs.

Immunoblotting Assay of VEGFR2 Signaling

VEGFR2 signaling in endothelial cells is primarily responsible for tumor angiogenesis. To investigate the angiogenic mechanism of BiSdAb C21–1 + 3VGR19–3 in HUVEC cells, we screened essential kinases involved in the VEGFR2 signaling pathway. Further, the phosphorylation of VEGFR2 and downstream signaling proteins were examined. The results showed that C21–1 + 3VGR19–3 inhibited VEGF-induced tyrosine phosphorylation of VEGFR2 and AKT/ERK/P38 MAPKs (►**Fig. 6**) in a dose-dependent manner. When 200 - nmol/L drugs was added, the percentages of p-VEGFR2/AKT/ERK/P38 MAPK compared with the total proteins were 5.43, 47.04, 10.69, and 15.12%, respectively ($p < 0.05$), as calculated by Image J software.

NK Cell Cytotoxicity Mediated by BiSdAb

Human NK cells were next used to assess the killing activity mediated by BiSdAb on VEGFR2+ cells BEL-7402. LDH release was measured to evaluate the cell cytotoxicity ratio (%). The results (►**Fig. 7**) indicate that 3VGR19–3 and C21–1 + 3VGR19–3 showed higher cytotoxicity at 48.6 and 78.7%

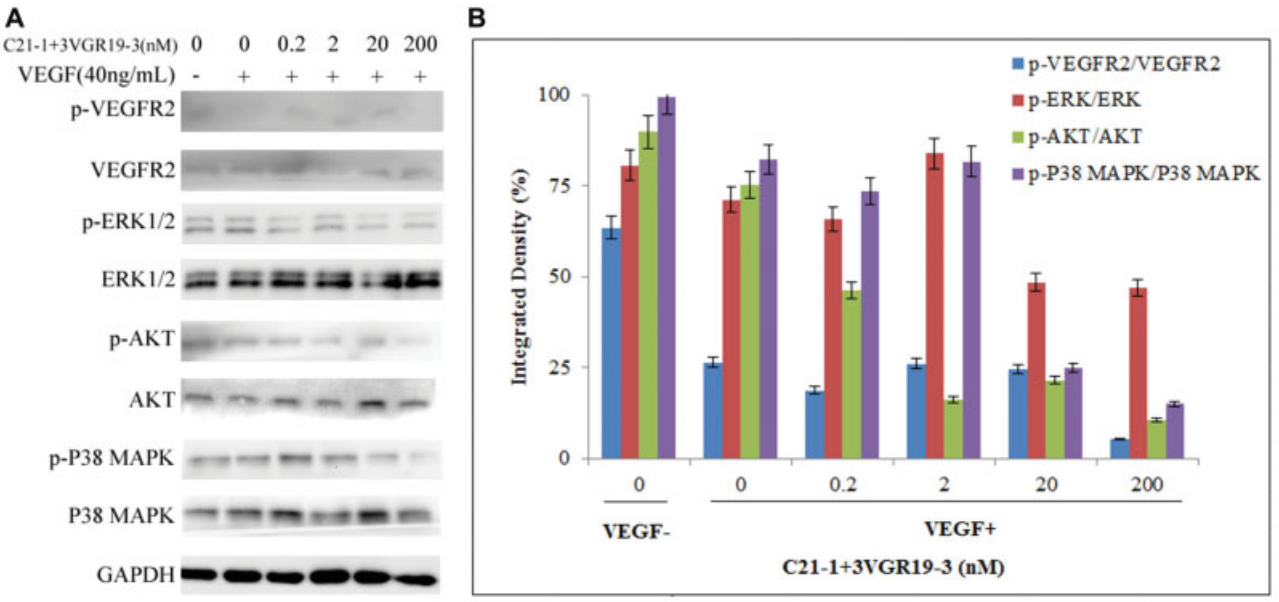

Fig. 6 (**A**) Western blot analysis for p-VEGFR2/VEGFR2, p-AKT/AKT, p-ERK/ERK, and p-P38/P38 in HUVECs treated with 3VGR19–3. Equal loading of protein was confirmed by stripping the immunoblot and reporting it for GAPDH. (**B**) Gray scanning and data statistics of (A). The data represent the mean of the triplicate experiments.

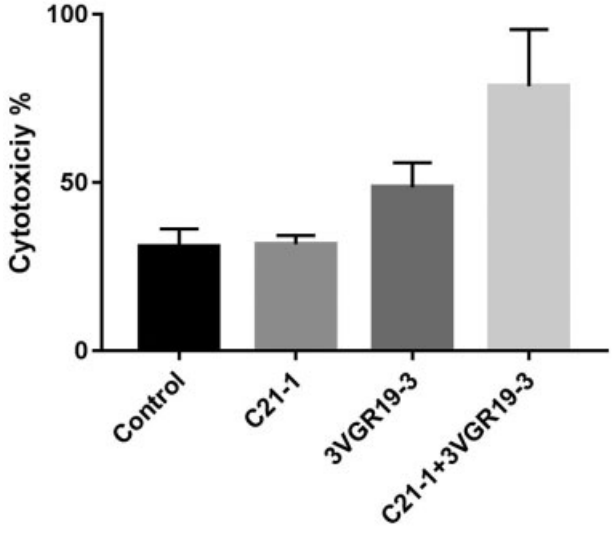

Fig. 7 NK cell cytotoxicity induced by SdAb and BiSdAb to target cell BEL-7402. NK, natural killer.

($p < 0.05$), respectively, than the PBS (31.0%) and C21–1 (31.7%) control groups. Thus, our BiSdAbs successfully induce NK cell killing.

Discussion

Cancer immunotherapy has generated great interest due to its potent therapeutic applications on cancer. Antiangiogenesis treatment, through blocking the interaction between VEGFs and VEGFRs, was proven to be an effective treatment for solid tumors. VEGFR2-targeted fusion antibody (mAb04-MICA) enhanced NK-mediated immunosurveillance against K562 leukemia cells.[33] Behdani and collaborators generated a functional SdAb 3VGR19 against the VEGFR2,[35] and Behar and collaborators isolated anti-CD16 SdAb C21 which activated NK cells.[37] In this report, we generated a novel BsAb based on a SdAb structure, named BiSdAb, for characterization of potential applications in cancer immunotherapy. Anti-VEGFR2 SdAb 3VGR19 and anti-CD16a SdAb C21 were successfully assembled and characterized biochemically and biologically.

In animal experiments, repeated administration of SdAb did not cause humoral or cellular immune response due to potential immunogenicity if used for a long time.[40] We conducted humanization of the antibody sequences to reduce potential immunogenicity caused by the BiSdAb. Acceptable affinities of the BiSdAbs toward corresponding targets were achieved.

Next, biological activities or anticancer activities in vitro were evaluated by cell proliferation, wound healing, endothelial tube formation, and apoptosis assays. BiSdAbs inhibited HUVEC cell proliferation in a dose-dependent manner, with an IC_{50} value of approximately 5.9 to 13.4 nmol/L (►**Fig. 4A**). SdAb 3VGR19–3 and C21–1 + 3VGR19–3 strongly inhibited HUVEC cell migration (►**Fig. 4B**). HUVECs grown in the presence of 3VGR19–3 and C21–1 + 3VGR19–3 formed fewer capillary tubes than those grown in vehicle media. Therefore, 3VGR19–3 and C21–1 + 3VGR19–3 had antiangiogenic effects on HUVEC tube formation. Treatment with BiSdAbs markedly increased apoptosis in HUVEC cells (from 26.81 to 59%). These observations collectively suggest that BiSdAbs demonstrated biological function of inhibition of cell proliferation, migration, endothelial tube formation, and angiogenesis in vitro. For the potential effect on tumor growth, we tried HCC BEL-7402 (►**Supplementary Fig. S4** [online only]), and the results showed that BiSdAb inhibited cell migration as a positive starting point for future studies of antitumor activities. Furthermore, we found that C21–

1 + 3VGR19–3 inhibited VEGF-induced phosphorylation of VEGFR2 and AKT/ERK/P38 MAPKs. Finally, NK cell cytotoxicity mediated by BiSdAb reached a high level of 78.7%. These results suggest that our BiSdAbs are promising candidates for further evaluation in animal models and eventually in humans.

Most of the investigational BsAb drugs are designed to recruit T cells to kill tumor cells, or simultaneously target two different cell surface receptors.[47] CD16 (FcγRIII) also plays an important role in mediating ADCC,[48] which could be linked to bring NK cells (via CD16) to attack cancer cells. Many BiKEs and TriKEs that specifically target CD16 expressed on effector NK cells and antigens on tumor cells are being developed and tested for clinical use. Our in vitro results suggest that BiSdAbs retained the affinity for VEGFR2 and CD16a, with selective binding and antiangiogenic activities. The ability of BiSdAbs to recruit NK cells to directly kill tumor cells in vivo will be interesting to address in future studies. As performed by Dong and collaborators, a BiSdAb by linking two SdAbs, anti-CEA and anti-CD16, was constructed in tandem. By recruiting NK cells to carcinoembryonic antigen positive cancer cells, this BiSdAb exhibited anticancer activity in vitro, as well as significantly suppressed cancer progression in xenograft models.[49]

Studies showed that anticancer activities of angiogenesis inhibitors could be strengthened by combination with other anticancer drugs.[50] Behdani et al fused a VEGFR2-specific SdAb to the truncated form of *Pseudomonas* exotoxin A and evaluated its ability to bind VEGFR2 on the cell surface. They demonstrated that the immunotoxin inhibits the proliferation of VEGFR2-expressing cells in vitro.[51] Thus, immunotoxin with BiSdAb should be interesting to evaluate in vivo as well.

Conclusions

In summary, our data suggest that the novel BiSdAb retained the high affinity, selective binding property, antiangiogenic activity, and cytotoxicity to cancer cells. It is a promising new approach to engaging NK cell-based immunotherapy for the treatment of solid tumors overexpressing VEGFR2. The results reported here form a base for further studies in in vivo animal studies aiming at solid tumor treatment.

Author Contributions

X.L. designed and conducted the experiments, analyzed the data, and drafted the manuscript; T.S. and Q. G. performed some of the experiments. J.Z. supervised project, analyzed data, critically discussed, and revised the manuscript. All authors read and approved the final manuscript.

Funding

This work was supported by the China Postdoctoral Science Foundation (2016M600319) and Natural Science Foundation of China (81473127&81773621).

Conflicts of Interest

The authors declare no conflict of interest.

Acknowledgments

The authors would like to thank Prof. Juan Zhang at State Key Laboratory of Natural Medicines, School of Life Science & Technology, China Pharmaceutical University, Nanjing, China, for providing NK92-FcR cells. The authors would like to thank Prof. Jinye Wang at School of Biomedical Engineering, Shanghai Jiao Tong University, for proving cell line BEL-7402. We would like to thank Dr. Jianrong Xu of Basic Medicine faculty at Shanghai Jiao Tong University for his assistance in affinity analysis by Biacore T200.

References

1 Weiner GJ. Building better monoclonal antibody-based therapeutics. Nat Rev Cancer 2015;15(06):361–370
2 Sharma P, Hu-Lieskovan S, Wargo JA, Ribas A. Primary, adaptive, and acquired resistance to cancer immunotherapy. Cell 2017;168 (04):707–723
3 Klinger M, Benjamin J, Kischel R, Stienen S, Zugmaier G. Harnessing T cells to fight cancer with BiTE® antibody constructs–past developments and future directions. Immunol Rev 2016;270(01): 193–208
4 Han L, Chen J, Ding K, et al. Efficient generation of bispecific IgG antibodies by split intein mediated protein trans-splicing system. Sci Rep 2017;7(01):8360
5 Wu Z, Cheung NV. T cell engaging bispecific antibody (T-BsAb): from technology to therapeutics. Pharmacol Ther 2018;182:161–175
6 Godar M, de Haard H, Blanchetot C, Rasser J. Therapeutic bispecific antibody formats: a patent applications review (1994-2017). Expert Opin Ther Pat 2018;28(03):251–276
7 Frampton JE. Catumaxomab: in malignant ascites. Drugs 2012;72 (10):1399–1410
8 Przepiorka D, Ko CW, Deisseroth A, et al. FDA approval: blinatumomab. Clin Cancer Res 2015;21(18):4035–4039
9 Scott LJ, Kim ES. Emicizumab-kxwh: first global approval. Drugs 2018;78(02):269–274
10 Thakur A, Huang M, Lum LG. Bispecific antibody based therapeutics: Strengths and challenges. Blood Rev 2018;32(04):339–347
11 Sedykh SE, Prinz VV, Buneva VN, Nevinsky GA. Bispecific antibodies: design, therapy, perspectives. Drug Des Devel Ther 2018; 12:195–208
12 Nuñez-Prado N, Compte M, Harwood S, et al. The coming of age of engineered multivalent antibodies. Drug Discov Today 2015;20 (05):588–594
13 Klingemann H, Boissel L, Toneguzzo F. Natural killer cells for immunotherapy - advantages of the NK-92 cell line over blood NK cells. Front Immunol 2016;7:91
14 Rezvani K, Rouce RH. The application of natural killer cell immunotherapy for the treatment of cancer. Front Immunol 2015;6:578
15 Ferrari de Andrade L, Tay RE, Pan D, et al. Antibody-mediated inhibition of MICA and MICB shedding promotes NK cell-driven tumor immunity. Science 2018;359(6383):1537–1542
16 Smits NC, Coupet TA, Godbersen C, Sentman CL. Designing multivalent proteins based on natural killer cell receptors and their ligands as immunotherapy for cancer. Expert Opin Biol Ther 2016;16(09):1105–1112
17 Chen S, Li J, Li Q, Wang Z. Bispecific antibodies in cancer immunotherapy. Hum Vaccin Immunother 2016;12(10):2491–2500
18 Wu J, Fu J, Zhang M, Liu D. AFM13: a first-in-class tetravalent bispecific anti-CD30/CD16A antibody for NK cell-mediated immunotherapy. J Hematol Oncol 2015;8:96
19 Pahl J, Reusch U, Gantke T, et al. AFM13 is the most advanced bispecific NK-cell engaging antibody in clinical development substantially enhancing NK-cell effector function and proliferation. Blood 2016;128:1764

20 Ferrara N, Kerbel RS. Angiogenesis as a therapeutic target. Nature 2005;438(7070):967–974
21 Carmeliet P, Jain RK. Angiogenesis in cancer and other diseases. Nature 2000;407(6801):249–257
22 Abdullah SE, Perez-Soler R. Mechanisms of resistance to vascular endothelial growth factor blockade. Cancer 2012;118(14):3455–3467
23 Ferrara N, Hillan KJ, Gerber HP, Novotny W. Discovery and development of bevacizumab, an anti-VEGF antibody for treating cancer. Nat Rev Drug Discov 2004;3(05):391–400
24 Verdaguer H, Tabernero J, Macarulla T. Ramucirumab in metastatic colorectal cancer: evidence to date and place in therapy. Ther Adv Med Oncol 2016;8(03):230–242
25 Hamers-Casterman C, Atarhouch T, Muyldermans S, et al. Naturally occurring antibodies devoid of light chains. Nature 1993;363 (6428):446–448
26 Allegra A, Innao V, Gerace D, Vaddinelli D, Allegra AG, Musolino C. Nanobodies and cancer: current status and new perspectives. Cancer Invest 2018;36(04):221–237
27 Steeland S, Vandenbroucke RE, Libert C. Nanobodies as therapeutics: big opportunities for small antibodies. Drug Discov Today 2016;21(07):1076–1113
28 Kijanka M, Dorresteijn B, Oliveira S, van Bergen en Henegouwen PM. Nanobody-based cancer therapy of solid tumors. Nanomedicine (Lond) 2015;10(01):161–174
29 Unciti-Broceta JD, Del Castillo T, Soriano M, Magez S, Garcia-Salcedo JA. Novel therapy based on camelid nanobodies. Ther Deliv 2013;4(10):1321–1336
30 Hassanzadeh-Ghassabeh G, Devoogdt N, De Pauw P, Vincke C, Muyldermans S. Nanobodies and their potential applications. Nanomedicine (Lond) 2013;8(06):1013–1026
31 Ayyar BV, Arora S, O'Kennedy R. Coming-of-age of antibodies in cancer therapeutics. Trends Pharmacol Sci 2016;37(12):1009–1028
32 Duggan S. Caplacizumab: first global approval. Drugs 2018;78 (15):1639–1642
33 Ren X, Xie W, Wang Y, et al. VEGFR2-targeted fusion antibody improved NK cell-mediated immunosurveillance against K562 cells. Immunol Res 2016;64(04):1060–1070
34 Xie W, Liu F, Wang Y, et al. VEGFR2 targeted antibody fused with MICA stimulates NKG2D mediated immunosurveillance and exhibits potent anti-tumor activity against breast cancer. Oncotarget 2016;7(13):16445–16461
35 Behdani M, Zeinali S, Khanahmad H, et al. Generation and characterization of a functional Nanobody against the vascular endothelial growth factor receptor-2; angiogenesis cell receptor. Mol Immunol 2012;50(1–2):35–41
36 Ma L, Gu K, Zhang CH, et al. Generation and characterization of a human nanobody against VEGFR-2. Acta Pharmacol Sin 2016;37 (06):857–864
37 Behar G, Sibéril S, Groulet A, et al. Isolation and characterization of anti-FcgammaRIII (CD16) llama single-domain antibodies that activate natural killer cells. Protein Eng Des Sel 2008;21 (01):1–10
38 Geng S, Wang Y, Wang L, et al. A light-responsive self-assembly formed by a cationic azobenzene derivative and SDS as a drug delivery system. Sci Rep 2017;7:39202
39 Lefranc MP, Ehrenmann F, Ginestoux C, Giudicelli V, Duroux P. Use of IMGT(®) databases and tools for antibody engineering and humanization. Methods Mol Biol 2012;907:3–37
40 Vincke C, Loris R, Saerens D, Martinez-Rodriguez S, Muyldermans S, Conrath K. General strategy to humanize a camelid single-domain antibody and identification of a universal humanized nanobody scaffold. J Biol Chem 2009;284(05):3273–3284
41 Lo BK. Antibody humanization by CDR grafting. Methods Mol Biol 2004;248:135–159
42 Biasini M, Bienert S, Waterhouse A, et al. SWISS-MODEL: modelling protein tertiary and quaternary structure using evolutionary information. Nucleic Acids Res 2014;42(Web Server issue): W252-8
43 Pardon E, Laeremans T, Triest S, et al. A general protocol for the generation of nanobodies for structural biology. Nat Protoc 2014; 9(03):674–693
44 Saerens D, Pellis M, Loris R, et al. Identification of a universal VHH framework to graft non-canonical antigen-binding loops of camel single-domain antibodies. J Mol Biol 2005;352(03):597–607
45 Könning D, Zielonka S, Grzeschik J, et al. Camelid and shark single domain antibodies: structural features and therapeutic potential. Curr Opin Struct Biol 2017;45:10–16
46 Kim JH, Hong HJ. Humanization by CDR grafting and specificity-determining residue grafting. Methods Mol Biol 2012; 907:237–245
47 Spiess C, Zhai Q, Carter PJ. Alternative molecular formats and therapeutic applications for bispecific antibodies. Mol Immunol 2015;67(2, Pt A):95–106
48 Cerwenka A, Lanier LL. Natural killers join the fight against cancer. Science 2018;359(6383):1460–1461
49 Dong B, Zhou C, He P, et al. A novel bispecific antibody, BiSS, with potent anti-cancer activities. Cancer Biol Ther 2016;17(04): 364–370
50 Folkins C, Man S, Xu P, Shaked Y, Hicklin DJ, Kerbel RS. Anticancer therapies combining antiangiogenic and tumor cell cytotoxic effects reduce the tumor stem-like cell fraction in glioma xenograft tumors. Cancer Res 2007;67(08):3560–3564
51 Behdani M, Zeinali S, Karimipour M, et al. Development of VEGFR2-specific nanobody Pseudomonas exotoxin A conjugated to provide efficient inhibition of tumor cell growth. N Biotechnol 2013;30(02):205–209